Shahid Beheshti University

Sustainable Earth Review

Journal homepage: http://sustainearth.sbu.ac.ir

Machine Learning Models for Estimating Actual Evapotranspiration with Limited Data

Adeeba Ayaz[a], Sharath Chandra Vannam[a], Shailesh Kumar Singh[b], Rehana Shaik[a*]

[a] Hydroclimatic Research Group, Lab for Spatial Informatics, International Institute of Information Technology Hyderabad (IIITH), India
[b] National Institute of Water and Atmospheric Research, Christchurch, New Zealand

ABSTRACT

The present study compared various empirical and data-driven algorithms to predict Actual Evapotranspiration (AET) using various hydro climatic variables. The AET over semi-arid climatic conditions of Hyderabad, Telangana, India, and Waipara (New Zealand) was estimated using different empirical methods-based PET using Budyko and Turc models. Modelled PET from five data-driven algorithms, such as Long short-term memory neural networks (LSTM), Artificial Neural Network (ANN), Gradient Boosting Regressor, Random Forest, and Support Vector Regression were trained to predict AET using meteorological variables. The results show simple empirical-based AET models, Budyko and Turc, can estimate AET very well. The results indicated that 99% accuracy could be achieved with all climatic input, whereas accuracy drops to 86% with limited data. Both LSTM and ANN models based on PET have been noted as the most robust models for estimating AET with minimal climate data. It was observed that the meteorological variables of temperature and solar radiation have more significant contributions than other variables in the estimation of AET. In addition, the effects of the meteorological variables were found to be essential and effective in the estimation of AET. The research findings of the study reveal that under limited data availability, the best input combinations were identified as temperature and wind speed for estimating PET; temperature, wind speed, and precipitation for estimating AET for semi-arid climatology.

ARTICLE INFO

Keywords:
AET
Evapotranspiration
PET

Article history:
Received: 05 Jan 2022
Accepted: 09 Mar 2022

*corresponding author
E-mail address:
rehana.s@iiit.ac.in
(R. Shaik)

1. Introduction

The complexity and variability of evapotranspiration processes in time and space have imposed some constraints on previously developed evapotranspiration models. Evapotranspiration (ET) is the combination of two processes where water is lost on one hand from the soil surface by evaporation and on the other hand from vegetation by transpiration (Chow, 2010). Availability of energy and water, and the ability to transport water vapour through the atmosphere affect the rate of evaporation, while the availability of energy, vapor pressure deficit and the amount of soil moisture control the transpiration rate (Bastiaanssen et al., 1998; Biggs et al., 2008; Su, 2002).

The quantity of water per unit time that evapotranspirates from a reference crop surface which has sufficient water is called reference crop evapotranspiration (Allan et al., 1998). A key aspect of the water budget is estimates of the spatial and temporal values of PET. PET is the enormous water flux representing the climatic demand of the water and the second most significant component of the terrestrial hydrological cycle next to rainfall. It is the process of returning water to the atmosphere via evaporation from open water, soil, and plant surfaces, as well as transpiration from plants. This term has been studied and modelled using different empirical methods and ML (Machine Learning) models. The methods for PET estimation is divided into physically based Penman-Monteith method (Allan et al., 1998).

The energy balance based methods Priestley-Taylor (Priestley and Taylor, 1972), Turc (Turc, 1961) and the temperature based Hargreaves method (Hargreaves and Samani, 1985). The uncertainties in PET estimates limit the reliability of hydrologic and restoration analyses, water resources management, and planning. Along with PET estimates, hydrological implications necessitate Actual Evapotranspiration (AET) estimates as well to get an actual water budget. AET expresses the annual water balance between precipitation and latent heat exchange, which is the variable most frequently correlated with biodiversity at the continental scales. Because of the close relationship between production and climatic factors, AET is also regarded as a surrogate for net primary production(Leith, 1975). Most studies in the literature have focused on modelling the PET process, in which evaporation occurs from soil and plant surfaces u er no water stress. However, AET occurs under actual water supply conditions. Earlier studies have estimated AET using time-consuming and labour-intensive methods such as water balance, energy balance, Bowen-ratio (EBBR), eddy-covariance (EC), and a few modelled-based methods. The modelled-based methods include Thornthwaite and Mather equation, Coutagne, Penman, Serra, Campus, Kessler, Jensen, and Haise, Blaney and Criddle, and Papadakis (Gudulas et al., 2013). These methods are empirical and the common issue in these methods is the calculation of certain components of the water balance based on several factors such as temperature, precipitation, humidity, etc. So, the need to estimate AET using limited data has become important. The Budyko and Turc methods appear to be the most appropriate; however, their application is heavily influenced by the regional conditions prevalent in each area. Furthermore, the more sensitive an area or station and the corresponding environmental pressures, the more important it is to apply the appropriate methods for estimating the important terms of the hydrological cycle and developing an efficient water resources management plan. This study adjusts the estimated PET values for the generation of AET. There are several studies that attempted to estimate AET using various empirical methods. However, estimation of AET using the PET estimates in the context of limited data availability has not been addressed. The present study tried to estimate AET for two different climatological conditions of Hyderabad and Waipara in the context of limited data which can serve as input to hydrological models of ungauged river basins. In this context, estimating AET given the PET estimates under limited data availability will be valuable in the water balance assessment studies for ungauged basins.

2. Material and Methods

2.1. Data and Case study

The present study selected two weather stations with diverse climatology of dry and wet conditions. One is Hyderabad, with distinct tropical wet and dry climate that borders on hot semi-arid (Köppen climate classification BSh). (https://en.wikipedia.org/wiki/Geography_of_ Hyderabad). Hyderabad is also the capital state of Telangana, which lies between latitude 17.366 N and longitude 78.746 E in the Deccan plateau with a normal stature of 536 m above mean sea level, possessing 650 square kilometres along the banks of Musi River with a populace of 9.75 million (Figure 1). The daily meteorological data were acquired from January 1965 through December 2015 (51 years) (612 months) from the weather station at Professor Jayashankar Telangana State Agricultural University, Rajendranagar, Hyderabad, India. The annual average weather data of the meteorological station is introduced in Table 1 for the Hyderabad station. Five meteorological variables were recorded at daily time scale, including (1) Maximum Air Temperature (Tx °C); (2) minimum Air Temperature (Tn °C); (3) minimum Relative Humidity (RH, %); (4) Wind Speed (U2, m s^{-1}) and (5) Solar Radiation (Rs, MJ m^{-2} d^{-1}). Measurements were carried out at 2 m (Air Temperature and Relative Humidity) and 10 m (Wind Speed) above the soil's surface. Data on Wind Speeds at 2 m (U2) were obtained from those taken at 10 m using the log-wind profile equation.

Table 1. Statistical values of available meteorological variables and ET_0 at Hyderabad station.

Parameters	Tx (°C)	Tn (°C)	RH (%)	Rs (W/m²)	U2 (m/s)	ET_0 (mm/day)
Maximum	45.50	33.00	100.00	14.45	189.90	13.16
Minimum	17.60	5.00	6.00	3.55	0.00	0.005
Mean	32.37	19.88	78.43	9.32	6.27	3.76
Standard deviation	4.10	4.79	14.48	2.44	6.18	1.72

Table 2. Statistical values of available meteorological variables and ET_0 at Waipara station.

Parameters	Tx (°C)	Tn (°C)	RH (%)	Rs (W/m²)	U2 (m/s)	ET_0 (mm/day)
Maximum	24.32	24.15	93.54	47.00	272.82	7.247
Minimum	−3.00	−3.00	0.00	0.00	0.00	0.00
Mean	10.17	9.95	65.61	15.29	1.75	1.50
Standard deviation	4.92	4.88	15.27	10.11	0.82	1.18

Table 3. Climate classification of Hyderabad and Waipara stations

Station	Precipitation	PET	P/PET (calculated)	P/PET (original)
Hyderabad	384.24	434.42	0.33	0.2-0.5 (semi-arid)
Waipara	146.98	1596.38	0.24	0.2-0.5 (semi-arid)

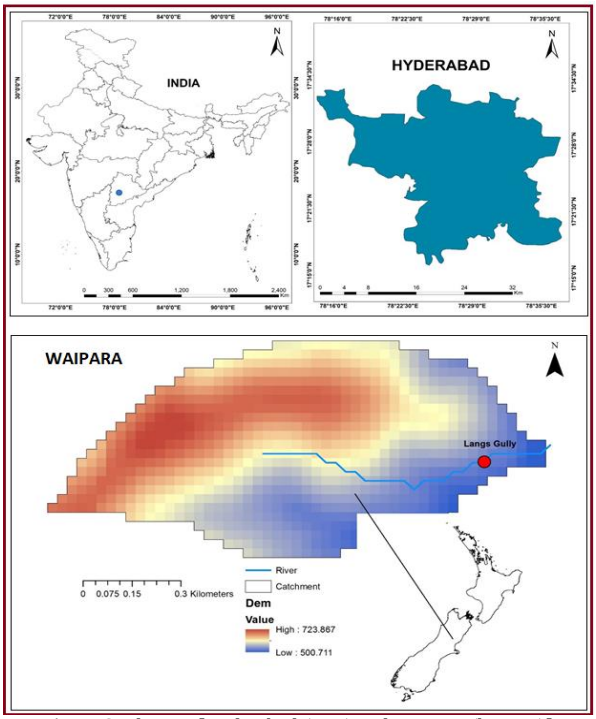

Fig. 1. Study area [Hyderabad (Top) and Waipara (bottom)].

The other station is Waipara experimental catchment (WARVEX) which is set up in Langs gully, situated on the South Island of New Zealand, in the Waipara River (Figure 1). The climate in the area is characterized by equable climates with few temperature extremes and abundant precipitation throughout the year. This climate's Koppen Climate Classification subtype is "Cfb". (West Coast Marine Climate). (https://www.weatherbase.com/weather/weather.php3?s=596172&cityname=Waipara-Canterbury-New-Zealand). The annual average weather data of the meteorological stations are given in Table 2 for the Waipara station and climate data was provided in Table 3. The catchment area of the Langs gully is 0.7 km^2. The elevation varies between 500 m and 723 m above sea level. The annual rainfall varies from 500 to 1100 mm/yr. It contains a surface slope of 0.22–34 degrees with a mean slope of 17 degrees. Soils are gravelly sandy loam, depth ranges from 0.25 to 1.5 m, and averages 0.5 m. Grass and exotic forests are the primary vegetation. An ephemeral stream flows from late March through early November. The catchment has regular frosts and occasional snow in winter. Field data from Lang gully was collected from 2010 to 2016. All data were stored in data loggers and had temporal resolutions of 10 minutes and have been

aggregated to the hourly time series for this study to match the model time step. In reference to the comparison of precipitation and PET, it was observed that both the stations fall under semi-arid regions (Table 3). Based on the Food and Agriculture Organization, Agro-Ecological Zone concept, classifies parts of the world as semi-arid if the annual precipitation totals between one fifth and one half of the PET (i.e., $0.2 < P/PET \leq 0.5$) from Table 3. It is the climate of a region with precipitation is less than PET but not as low as a desert climate.

2.2. Methodology

Estimation of Potential Evapotranspiration using Empirical Methods:

PET can be estimated based on energy balance and water vapor mass flux transfer based empirical methodologies (Ma et al., 2021). These empirical models vary in terms of solar radiation, temperature considering the physical processes of radiation, and transport characteristics of natural surfaces**.**

FAO-Penman Monteith Method:

The Food and Agriculture Organization of the United Nations (FAO) suggested that the Penman Monteith as widely used worldwide as benchmark evapotranspiration assessment (Allan et al., 1998). Estimation of PET using Penman-Monteith model, various climatic factors, including temperature, wind speed, solar radiation, and relative humidity, are required (Eq. 1).

$$PET = \frac{0.408D(Rn-G)+g\left(\frac{900}{T+273}\right)U2(es-ea)}{D+g(1+0.34U2)} \quad (1)$$

Where *Rn* is the net radiation at crop surface (MJ m^{-2} d^{-1}), *G* is the soil heat flux (MJ m^{-2} d^{-1}), *T* is the average temperature at 2 m height(°C), *U2* is wind speed measured at 2 m height [m s^{-1}], *(es - ea)* is pressure deficit for measurement at 2 m height [k Pa], *D* is slope vapor pressure curve [k pa°C^{-1}],*g* is psychrometric constant [k pa°C^{-1}],900 is coefficient for the reference crop [l J^{-1} Kg K d^{-1}], 0.34 is wind coefficient for the reference crop [s m^{-1}].

Turc Method:

Turc developed an equation (Turc, 1961) for calculating daily PET as a function of air temperature, relative humidity, and solar radiation. The Turc method estimates PET based on mean temperature and solar radiation on the daily time scale. The equation is given by Eq. 2.

$$PET = 0.013\frac{Tm}{Tm+15}(23.88Rs + 50) \quad (2)$$

Where *Tm* is the mean temperature (°C), solar radiation (*Rs*) is [0.25 + 0.5 (*n/N*)] *Ra*, *Ra* is extra-terrestrial radiation (mm⁄d), *n* is actual hours of bright sunshine (hrs), *N* is the maximum possible hours of sunshine (hrs).

Priestly and Taylor method:

The Priestley-Taylor model is a condensed version of the original Penman combination equation, which was developed by (Priestley and Taylor, 1972). The model original purpose was to be used in large-scale numerical modelling where it is assumed that because advection is negligible, the aerodynamic component of the original Penman equation can be ignored. This method is calculated using net radiation and latent heat of vaporization on a daily time scale. The equation is given by Equation 3.

$$PET = A\left(\frac{D}{D+g}\right)\left(\frac{Rn-G}{L}\right)$$

$$D=\frac{4098[0.6108exp(\frac{17.27*Tm}{Tm+237.3})]}{(Tm+237.3)^2} \quad (3)$$

Where *D* is slope vapor pressure curve [k pa°C-1], *g* is psychrometric constant [k pa°C-1], *Rn* is the net radiation at crop surface (MJ m-2 d -1), *A* is a calibration constant 1.26, *L* is the latent heat of vaporization and can be considered as 2.45 (MJ/kg) which is constant.

Hargreaves Method:

The Hargreaves-Samani model is one of the more well-known versions of an older evapotranspiration model (Hargreaves and Samani, 1985). The Hargreaves-Samani method estimates PET based on maximum and minimum air temperature on a daily time scale. The equation is given by Equation 4.

$$PET=0.0023Ra\,(Tm+17.8)\,(Td^{0.5} \quad (4)$$

Where, *Td* = difference between maximum temperature and min temperature (°C), *Tm* = mean temperature (°C), *Ra* = extra-terrestrial radiation (mm⁄d)

Estimation of Actual Evapotranspiration using Empirical methods:

AET is constrained by the availability of energy, water, and the resistance provided by the atmosphere and vegetation (Rim, 2008). Because of these constraints, AET measurement methodologies such as micrometeorological methods (energy-budget Bowen ratio or eddy correlation), and lysimeter-based techniques are costly and labour-intensive (Su et al., 2022). However, empirical models have been developed for estimating AET using precipitation and PET, which works on the assumption that AET is constrained by

precipitation under dry conditions and PET under wet conditions (Zhang et al., 2008). The present study has provided alternatives based on precipitation and PET equations to estimate AET under limited data conditions for two different climatic regions of Hyderabad and Waipara. The present study used classical empirical AET models, which uses the precipitation and PET as inputs such as Budyko (1974) and Turc (1954). The implementation of the proposed methodology was done based on the PET modelled using different machine learning models taking the Penman-Monteith as the reference method. The PET estimates from various ML models such as LSTM, ANN, RF, SVR, and GBR were utilized in place of PET in the Budyko and Turc methods. The meteorological variables used in estimating PET were temperature, wind speed, and relative humidity. The proposed methodology provides a detailed understanding on estimating AET with readily available PET and precipitation under limited data for diverse climatic conditions.

Budyko method:

To estimate AET with readily available and modelled operational hydro-meteorological variables of P and PET, the study adopted the Budyko (1961) equation. Budyko Equation is a classic model for estimating AET by relating long-term-average water and energy balances at catchment scales using precipitation and PET. Budyko established a relationship between three hydro-climatic variables for a basin: precipitation (P), PET, and AET. The Budyko formulation depends on the relationship between three hydro-meteorological variables: P, PET, and AET, which states that the ratio of the AET over precipitation (AET/P) is fundamentally related to the ratio of the PET over precipitation (PET/P) (Budyko, 1961; Fu, B.P., 1981) as follows Equation 5.

$$\frac{ET}{P} = 1 + \frac{PET}{P} - \left(1 + \left(\frac{PET}{P}\right)^{\omega}\right)^{(1/\omega)} \quad (5)$$

The parameter 'ω' Accounts for the basin characteristics such as soil, vegetation, terrain, etc.(McVicar et al., 2012). The original Budyko equation was developed for a long timescale. For a reasonable application of the Budyko equation for short-term scales, the original Budyko formulation has been modified by several researchers and one of the most widely used formulations is as implemented by (Zhang et al., 2008) for estimating the AET, as follows Equation 6.

$$AET_{Budyko} = \left[P\left(1 - exp\left(\frac{-PET}{P}\right)\right) PET\ tanh\left(\frac{P}{PET}\right)\right]^{0.5} \quad (6)$$

Turc Method:

Another well accepted and widely used AET model which considers precipitation and PET along with soil and vegetative characteristics implicitly is Turc model (Turc, 1954). It is also one of the widely used AET models in hydrological applications (e.g.(Asokan and Jarsjö, 2010) (Eq. 7).

$$AET_{Turc} = \frac{P}{\sqrt{0.9 + \frac{P^2}{PET^2}}} \quad (7)$$

2.3. Machine Learning Methods

In this study, four ML models were implemented for modelling PET for Hyderabad and Waipara stations, namely, LSTM, GBR, SVR, and RF regressor, and a comparison was made between the models to analyse the best ML model with limited meteorological data for two diverse climatic conditions.

2.3.1. Long short-term memory (LSTM)

Long short-term memory neural networks are like Recurrent neural networks (RNN), which have the capability to learn larger data compared to normal RNNs. This is done by controlling the hidden state in LSTM and solving the vanishing gradient problem. LSTM has feedback connections and an input gate, an output gate, and a forget gate (Figure 2). LSTM calculates a gate values by using the previous cell value C_{t-1}, previously hidden values h_{t-1}, and input x_t.

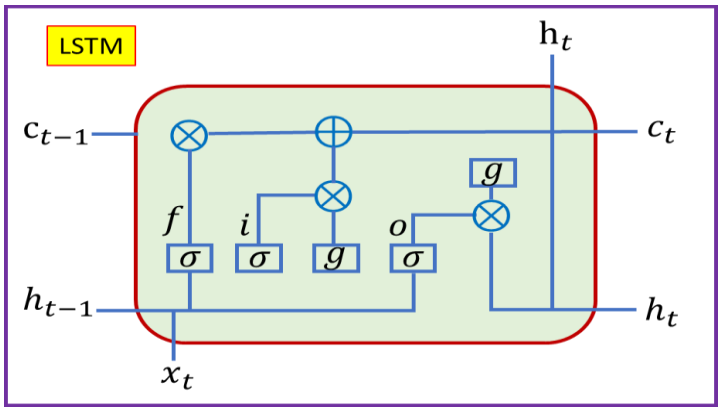

Fig. 2. Overview diagram of Long short-term memory (LSTM). Where *f, i and o* denotes the forget gate, input gate, an output gate, h_t denotes hidden state, C_t denotes cell state, σ is the sigmoid function, and g is the activation function.

$$i_t = F(W_{xi}x_t + W_{hi}h_{t-1} + W_{ci}C_{t-1} + bias_i)$$
$$o_t = F(W_{xo}x_t + W_{ho}h_{t-1} + W_{co}C_{t-1} + bias_o)$$
$$f_t = F(W_{xf}x_t + W_{hf}h_{t-1} + W_{cf}C_{t-1} + bias_f)$$

And the cell value is calculated using Equation 8.

$$C_t = f_tC_{t-1} + i_tF(W_{xc}x_t + W_{hc}h_{t-1} + bias_c)$$
$$h_t = o_t tanh(C_t) \quad (8)$$

LSTM is like RNN, but by using the three gates, it can process longer lengths of data, and it is also able to solve the vanishing gradient problem.

2.3.2. Gradient boosting regression (GBR)

GBR was introduced by (Geigy et al., 1975; Jensen et al., 2012), also known as multiple additive regression trees (MART) or Gradient boosting decision tree (GBDT), is used ML algorithm to get robust performance in practical applications. As defined by (Blaney and 1892, 1952), GBR comprises three elements: a loss function, a weak learner, and an additive model to optimize, make predictions, and add weak learners to minimize the loss function, respectively. Because GBR is fast, to avoid overfitting, it is good at handling missing values and outliers, and it is superior to conventional ML methods in many fields (Blaney and 1892, 1952; Bray and Kurtz, 1945). It also allows for the optimization of arbitrary differentiable loss functions. In each stage, a regression tree is fit on the negative gradient of the given loss function. Gradient boosting involves three elements: A loss function to be optimized, a weak learner to make predictions, and an additive model to add weak learners to minimize the loss function. Gradient Boosting is a greedy algorithm and can overfit a training dataset quickly. It can benefit from regularization methods that penalize various parts of the algorithm and improve the performance of the algorithm by reducing overfitting. There are four improvements to basic gradient boosting: Tree Constraints, Shrinkage, Sampling, and Penalized learning. Gradient Boosting trains many models in a gradual, additive, and sequential manner. The major difference between AdaBoost and Gradient Boosting Algorithms is how the two algorithms identify the shortcomings of weak learners (e.g., decision trees). While the AdaBoost model identifies the shortcomings by using high weight data points, gradient boosting performs the same by using gradients in the loss function (y = ax + b + e, e needs a special mention as it is the error term). The loss function is a measure indicating how good a model's coefficients are at fitting the underlying data. A logical understanding of loss function would depend on what we are trying to optimize. For example, if we are trying to predict the sales prices by using a regression, then the loss function would be based on the error between true and predicted house prices. Similarly, if our goal is to classify credit defaults, then the loss function would be a measure of how good our predictive model is at classifying bad loans. One of the biggest motivations for using gradient boosting is that it allows one to optimize a user-specified cost function, instead of a loss function that usually offers less control and does not correspond with real-world applications.

2.3.3. Random forest regression (RF)

RF is an ensemble technique, which is capable of both classification and regression, known as bagging. It is one of the practical algorithms for predictive analysis. In determining the final output, the principle of RF is to combine the

various decision trees rather than depending on individual decision trees. RF is used for classification by majority vote and regression by an average of the single-tree method in the output generation process (Jensen et al., 1990). RF models have supervised ML approaches, which are popular in ML and are frequently used in hydrology (Bray and Kurtz, 1945; Landeras et al., 2008; Walter et al., 2012). The Sum of Squared Error (SSE) has been calculated between the observed values and the predicted values. This procedure will recursively continue until the entire data is covered. The model can be written as Equation 9.

$$f(x) = f_o(x) + f_1(x) + f_2(x) + \cdots \quad (9)$$

Where the ultimate model f is the sum of simple base models f_i. Where each base regressor portion is the simple decision tree. The basic idea behind this is to combine multiple decision trees in determining the final output rather than relying on individual decision trees.

Approach: 1. Pick at random K data points from the training set; 2. Build the decision tree associated with those K data points; 3. Choose the number Ntree of trees you want to build and repeat steps 1 & 2; 4. For a new data point, make each one of your Ntree trees predict the value of Y for the data point, and assign the new data point the average across all the predicted Y values. Random forests or random decision forests are an ensemble learning method for classification, regression, and other tasks that operate by constructing a multitude of decision trees at training time and outputting the class that is the mode of the classes (classification) or mean prediction (regression) of the individual trees. Random decision forests correct for decision trees' habit of overfitting to their training set. Each Decision Tree in the Extra Trees Forest is constructed from the original training sample. Then, at each test node, each tree is provided with a random sample of k features from the feature-set from which each decision tree must select the best feature to split the data based on some mathematical criteria (typically the Gini Index). This random sample of features leads to the creation of multiple de-correlated decision trees.

2.3.4. Support vector regression (SVR)

In several research studies, SVR, which is focused on systemic risk minimization to prevent overfitting (Deo and Samui, 2016), was adopted over ANN due to the solution's uniqueness and globalization (Magliulo et al., 2003). The SVR has been commonly used in engineering (Alexandris and Kerkides, 2003; Naoum and Tsanis, 2003; Zheng et al., 2016) Its evapotranspiration applications are also quite impressive (Asokan and Jarsjö, 2010; Pereira and Pruitt, 2004; Utset et al., 2004) firstly, applied the SVR approach for rainfall-runoff modeling in hydrology. SVRs are today known as efficient and robust ML algorithms for predictions. When the training data of $\{(x_1,y_1), \ldots \ldots .. (x_n,y_n)\}$ with n patterns, a function $f(x)$ will be identified with the consideration of the deviation from the observed target variables y_i for all the training data (Silva and Manzione, 2021). Using a non-linear mapping function φ, X will map the input variables to a higher dimensional feature space.

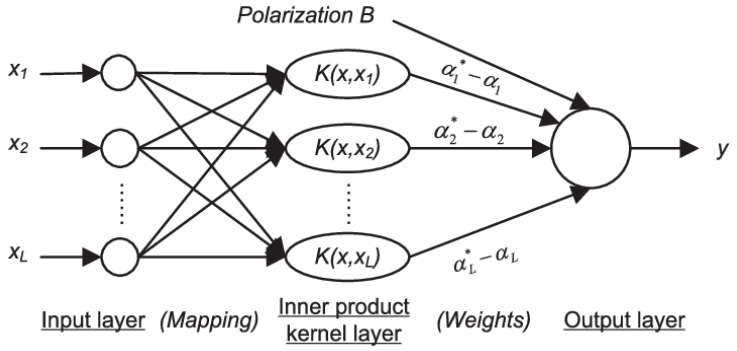

Fig. 3. Structure of Support Vector Regression

In simple regression, we try to minimize the error rate. While in SVR we try to fit the error within a certain threshold. Our objective with SVR is to consider the points that are within the boundary line. Our best fit line is the line hyperplane that has a maximum number of points. In the case of regression, a margin of tolerance (epsilon) is set in approximation to the SVM (Support Vector Machines) which would have already been requested from the problem.

But besides this fact, there is also a more complicated reason, the algorithm is more complicated and therefore to be taken into consideration. However, the main idea is always the same: to minimize error, individualizing the hyperplane which maximizes the margin, keeping in mind that part of the error is tolerated. The goal of linear regression is to minimize the error between the prediction and data. In SVR, the goal is to make sure that the errors do not exceed the threshold (Eq. 10).

$$f(x;w) =< W, \varphi(x) > +b \quad (10)$$

Where W and b are the regression coefficients and <, > denotes the inner product. SVR uses the $\in$ insensitive error to measure the error between $f(x)$ and the observed values of y, (Eq. 11).

$$|f(x;w)-y|_{\in} = \begin{cases} 0, & if\ |f(x;w)-y| < \in \\ |f(x;w)-y| - \in, & otherwise. \end{cases} \quad (11)$$

Using the training data of (x_i,y_i) the values of w and b are calculated by minimizing the objective function (Eq. 12):

$$F = \frac{C}{N}\sum_{i=1}^{n} |f(x_i,w)-y_i|_{\in} + \frac{1}{2}||w||^2 \quad (12)$$

Where $\in$ and C are the hyper-parameters. The minimization of the objective function, F, uses the Lagrange multiplier method. The ultimate regression equation with kernel function $K(X,X')$ can be in the form (Eq. 13).

$$f(X) = \sum_i K(X, X_i) + b \quad (13)$$

Based on earlier studies (Amatya et al., 1995), the kernel function RBF was chosen to measure the performance of the model for the ET_0. A complete overview of the SVR method can be found in (Amatya et al., 1995)

2.3.5. Model evaluation

The accuracy of the ML models was calculated using the coefficient of determination (R^2) (Eq. 14), the root mean squared error (RMSE) (Eq. 15), and the mean absolute error (MAE) (Eq. 16). The equations are as follows:

$$R^2 = 1 - \frac{\sum(ET_{obs}-ET_{sim})^2}{\sum(ET_{obs}-ET_{mean})^2} \quad (11)$$

$$RMSE = \sqrt{MSE} = \sqrt{\frac{\sum_{i=1}^{n}(ET_{obs}-ET_{sim})^2}{n}} \quad (12)$$

$$MAE = \frac{1}{N}\sum_{i=1}^{n}(ET_{obs} - ET_{sim}) \quad (13)$$

Where ET_{sim} is the simulated potential evapotranspiration, ET_0 at time step i in mm/day. ET_{obs} is the observed ET_0 at time step i in mm/day. ET_{mean} is the average ET_0 at time step i in mm/day. n is the number of data pairs, respectively.

3. Results and discussion

The modelled PET estimates using five different ML models like LSTM, GBR, RF, ANN, and SVR were considered in this analysis to estimate AET using Budyko and Turc methods. The climate variables considered for estimating daily PET using five different models and Penman-Monteith methods were the daily maximum temperature, minimum temperature, relative humidity, and solar radiation. The four various optimal input combinations for modelling this daily PET were all available meteorological parameters; temperature, wind speed, and relative humidity; temperature and wind speed; and temperature and relative humidity. The two AET methods of Budyko and Turc use precipitation, and the PET estimates. The input combinations were replicated from the estimation of PET to estimate different modelled combinations of AET as given in Tables 4-7. The best empirical AET methods were recorded corresponding to the four ML models and their input combinations in terms of R^2, RMSE, and MAE for four empirical methods. These were listed in Tables 4, 5, 6, and 7 for the Hyderabad and Waipara Stations.

Table 4. Performance of Budyko and Turc methods in estimating AET using PET modelled from Random Forest (RF), Support Vector Regressor (SVR), Gradient Boosting Regressor (GBR), Long Short-Term Memory (LSTM) and Artificial Neural Network (ANN) for Penman-Monteith Method under different input combinations.

Parameters	Model	Hyderabad						Waipara					
		Budyko			Turc			Budyko			Turc		
		R^2	RMSE (mm/d)	MAE (mm/d)	R^2	RMSE (mm/d)	MAE (mm/d)	R^2	RMSE (mm/d)	MAE (mm/d)	R^2	RMSE (mm/d)	MAE (mm/d)
All parameters	RF	0.99	0.05	0.01	0.99	0.06	0.01	0.99	0.03	0.04	0.99	0.02	0.01
	SVR	0.99	0.04	0.02	0.99	0.04	0.02	0.98	0.02	0.01	0.98	0.03	0.04
	GBR	0.99	0.09	0.02	0.99	0.09	0.02	0.98	0.03	0.04	0.99	0.03	0.04
	LSTM	0.99	0.05	0.01	0.99	0.06	0.01	0.95	0.22	0.01	0.97	0.23	0.05
	ANN	0.99	0.04	0.01	0.99	0.04	0.01	0.98	0.02	0.01	0.98	0.03	0.01

Temperature, Wind Speed, Relative Humidity	RF	0.91	0.51	0.17	0.91	0.18	0.26	0.95	0.06	0.01	0.95	0.06	0.01
	SVR	0.92	0.47	0.14	0.91	0.50	0.16	0.95	0.05	0.03	0.95	0.05	0.06
	GBR	0.91	0.47	0.14	0.91	0.45	0.15	0.95	0.05	0.01	0.96	0.06	0.01
	LSTM	0.92	0.38	0.09	0.92	0.49	0.15	0.96	0.19	0.05	0.96	0.20	0.05
	ANN	0.92	0.48	0.15	0.91	0.40	0.09	0.96	0.06	0.02	0.96	0.06	0.01
Temperature and Wind Speed	RF	0.90	0.69	0.26	0.89	0.72	0.27	0.79	0.19	0.05	0.79	0.20	0.05
	SVR	0.91	0.57	0.22	0.91	0.58	0.22	0.89	0.14	0.03	0.89	0.14	0.04
	GBR	0.92	0.56	0.21	0.91	0.58	0.22	0.85	0.17	0.05	0.85	0.18	0.05
	LSTM	0.92	0.52	0.18	0.93	0.59	0.23	0.77	0.21	0.06	0.77	0.22	0.06
	ANN	0.920	0.56	0.21	0.92	0.54	0.19	0.86	0.18	0.05	0.85	0.19	0.05
Temperature and Relative Humidity	RF	0.84	0.64	0.19	0.84	0.66	0.20	0.95	0.07	0.05	0.92	0.08	0.06
	SVR	0.88	0.54	0.18	0.88	0.60	0.21	0.92	0.05	0.07	0.95	0.06	0.07
	GBR	0.881	0.58	0.21	0.88	0.60	0.21	0.92	0.06	0.05	0.99	0.06	0.01
	LSTM	0.85	0.48	0.15	0.85	0.56	0.18	0.95	0.19	0.05	0.77	0.20	0.05
	ANN	0.88	0.58	0.20	0.87	0.50	0.15	0.95	0.06	0.01	0.95	0.06	0.01

Table 5. Performance of Budyko and Turc methods in estimating AET using PET modelled from Random Forest (RF), Support Vector Regressor (SVR), Gradient Boosting Regressor (GBR), Long Short-Term Memory (LSTM) and Artificial Neural Network (ANN) for Priestley Taylor Method under different input combinations.

		Hyderabad						Waipara					
Parameters	**Model**	**Budyko**			**Turc**			**Budyko**			**Turc**		
		R^2	**RMSE (mm/d)**	**MAE (mm/d)**	**R^2**	**RMSE (mm/d)**	**MAE (mm/d)**	**R^2**	**RMSE (mm/d)**	**MAE (mm/d)**	**R^2**	**RMSE (mm/d)**	**MAE (mm/d)**
All parameters	RF	0.94	0.09	0.02	0.94	0.20	0.03	0.93	0.04	0.04	0.93	0.04	0.05
	SVR	0.96	0.08	0.04	0.96	0.18	0.04	0.88	0.06	0.02	0.88	0.06	0.09
	GBR	0.96	0.06	0.02	0.96	0.01	0.01	0.88	0.06	0.03	0.88	0.06	0.03
	LSTM	0.99	0.01	0.022	0.99	0.03	0.024	0.92	0.05	0.03	0.92	0.05	0.08
	ANN	0.95	0.07	0.03	0.95	0.17	0.03	0.92	0.05	0.08	0.92	0.05	0.08
Temperature and Rs	RF	0.92	0.23	0.03	0.92	0.24	0.03	0.49	0.18	0.03	0.49	0.19	0.03
	SVR	0.93	0.22	0.06	0.93	0.23	0.06	0.53	0.16	0.03	0.53	0.17	0.03
	GBR	0.93	0.22	0.05	0.93	0.23	0.05	0.54	0.17	0.04	0.54	0.18	0.04
	LSTM	0.86	0.30	0.04	0.86	0.31	0.05	0.54	0.17	0.03	0.54	0.17	0.03
	ANN	0.93	0.21	0.05	0.93	0.22	0.05	0.53	0.17	0.03	0.53	0.18	0.03
Temperature and Relative Humidity	RF	0.89	0.26	0.04	0.89	0.28	0.04	0.58	0.16	0.03	0.57	0.17	0.03
	SVR	0.93	0.21	0.04	0.93	0.22	0.04	0.60	0.13	0.03	0.60	0.14	0.01
	GBR	0.93	0.22	0.03	0.92	0.23	0.04	0.60	0.15	0.03	0.60	0.16	0.03
	LSTM	0.97	0.11	0.02	0.97	0.63	0.12	0.03	0.15	0.03	0.61	0.16	0.03
	ANN	0.93	0.22	0.03	0.93	0.28	0.05	0.59	0.15	0.03	0.59	0.16	0.03

Table 6. Performance of Budyko and Turc methods in estimating AET using PET modelled from Random Forest (RF), Support Vector Regressor (SVR), Gradient Boosting Regressor (GBR), Long Short-Term Memory (LSTM) and Artificial Neural Network (ANN) for Hargreaves Method under different input combinations.

		Hyderabad						Waipara					
Parameters	**Model**	**Budyko**			**Turc**			**Budyko**			**Turc**		
		R^2	**RMSE (mm/d)**	**MAE (mm/d)**	**R^2**	**RMSE (mm/d)**	**MAE (mm/d)**	**R^2**	**RMSE (mm/d)**	**MAE (mm/d)**	**R^2**	**RMSE (mm/d)**	**MAE (mm/d)**
All parameters	RF	0.99	0.01	0.01	0.99	0.01	0.02	0.97	0.07	0.02	0.97	0.07	0.02
	SVR	0.98	0.04	0.02	0.98	0.04	0.02	0.99	0.02	0.06	0.99	0.02	0.06
	GBR	0.99	0.01	0.03	0.99	0.01	0.04	0.97	0.07	0.02	0.98	0.07	0.02
	LSTM	0.99	0.01	0.02	0.99	0.01	0.01	0.97	0.02	0.03	0.97	0.02	0.08
	ANN	0.99	0.01	0.03	0.99	0.01	0.01	0.99	0.02	0.07	0.99	0.02	0.08
Minimum Temperature , Rs	RF	0.99	0.25	0.05	0.99	0.29	0.05	0.97	0.04	0.08	0.97	0.07	0.05
	SVR	0.98	0.13	0.03	0.98	0.13	0.04	0.99	0.02	0.06	0.98	0.02	0.06
	GBR	0.99	0.13	0.02	0.98	0.13	0.02	0.99	0.06	0.02	0.99	0.07	0.02
	LSTM	0.99	0.20	0.02	0.99	0.21	0.02	0.97	0.02	0.04	0.97	0.02	0.04
	ANN	0.99	0.13	0.02	0.98	0.14	0.03	0.99	0.02	0.05	0.99	0.02	0.06

Table 7. Performance of Budyko and Turc methods in estimating AET using PET modelled from Random Forest (RF), Support Vector Regressor (SVR), Gradient Boosting Regressor (GBR), Long Short-Term Memory (LSTM) and Artificial Neural Network (ANN) for Turc Method under different input combinations.

		Hyderabad						Waipara					
		Budyko			Turc			Budyko			Turc		
Parameters	**Model**	**R^2**	**RMSE (mm/d)**	**MAE (mm/d)**	**R^2**	**RMSE (mm/d)**	**MAE (mm/d)**	**R^2**	**RMSE (mm/d)**	**MAE (mm/d)**	**R^2**	**RMSE (mm/d)**	**MAE (mm/d)**
All parameters	RF	0.99	0.02	0.01	0.99	0.04	0.05	0.99	0.06	0.04	0.99	0.06	0.04
	SVR	0.99	0.02	0.01	0.98	0.03	0.01	0.99	0.01	0.04	0.99	0.01	0.04
	GBR	0.99	0.04	0.04	0.99	0.05	0.04	0.99	0.01	0.04	0.99	0.01	0.04
	LSTM	0.99	0.01	0.02	0.99	0.01	0.03	0.99	0.02	0.01	0.99	0.02	0.01
	ANN	0.99	0.07	0.01	0.99	0.07	0.01	0.99	0.02	0.01	0.99	0.02	0.01
Minimum Temperature , Rs	RF	0.99	0.01	0.01	0.99	0.01	0.04	0.93	0.10	0.01	0.93	0.10	0.01
	SVR	0.98	0.02	0.04	0.98	0.02	0.04	0.99	0.08	0.01	0.99	0.09	0.01
	GBR	0.99	0.08	0.04	0.99	0.08	0.04	0.95	0.08	0.01	0.95	0.09	0.01
	LSTM	0.95	0.04	0.03	0.95	0.21	0.03	0.99	0.09	0.01	0.98	0.10	0.01
	ANN	0.99	0.08	0.04	0.99	0.08	0.01	0.99	0.09	0.01	0.99	0.10	0.01

The performance of AET methods (Budyko and Turc) using PET obtained from ML models such as LSTM, ANN, SVR, GBR, and RF and Penman-Monteith method for the two stations of Hyderabad and Waipara was provided in Table 4. The results demonstrated that the tested models had comparable performance over the two stations. Figure 4 shows the comparisons between observed AET using PET from Penman-Monteith and the AET estimated using modelled PET values with all parameters as input combinations. The model estimated values of AET using LSTM, ANN, and SVR based PET models showed closer agreement with observed AET estimates. Also during the testing period, the LSTM and ANN models performed marginally better than the GBR, with estimated R^2 values of the two stations being Hyderabad as 0.990 (LSTM), 0.998 (ANN), 0.990 (SVR) and 0.990 (GBR), 0.990 (RF) and for Waipara 0.990 (LSTM), 0.998 (ANN), 0.990 (SVR) and 0.990 (GBR), 0.990 (RF). For Hyderabad station, the results were the same for both the AET methods; it was seen that both Budyko and Turc performed well. It was also observed from the study that, among the evaluated models, LSTM and ANN models with all input combinations accomplished excellent performances, trailed by SVR. The performances for the models being LSTM (RMSE: 0.06 mm⁄d, MAE: 0.01 mm⁄d, and R^2: 0.990) for the Budyko method and (RMSE: 0.04 mm⁄d, MAE: 0.01 mm⁄d, and R^2: 0.998) for Turc method, ANN (RMSE: 0.04 mm⁄d, MAE: 0.01 mm⁄d, and R^2:0.998), SVR (RMSE: 0.04 mm⁄d, MAE: 0.02 mm⁄d, and R^2: 0.990), for Budyko as well as Turc methods. The GBR model could likewise accomplish reliable results with (RMSE: 0.09 mm⁄d, MAE: 0.02 mm⁄d, and R^2: 0.987), while the RF model had also shown promising performance with (RMSE: 0.05 mm⁄d, MAE: 0.01 mm⁄d, and R^2: 0.980).

The performances of the five ML models and the two AET methods for the Priestley Taylor method of PER was provided in Table 5. Table 5 demonstrated that the tested models had comparable performance over the two stations. Figures 5-6 show the comparisons between observed AET and model estimated values in the form of a box plot for two AET-based methods under different input combinations for both stations. From Table 5 for the Priestley Taylor method also results were the same with the models LSTM, ANN, and SVR estimated values showing closer agreement with those of observed AET followed by GBR and RF.

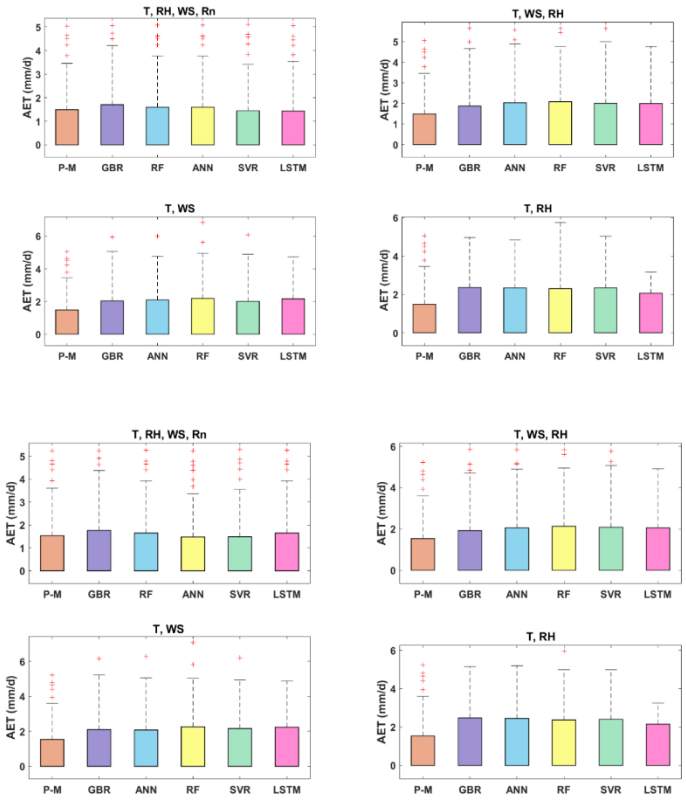

Fig. 4. Comparison of observed and estimated AET using different models (GBR, ANN, LSTM, RF, and SVR) with varying parameters of input for the validation period for Budyko (Top) and Turc methods (Bottom) at Hyderabad station for Penman-Monteith method.

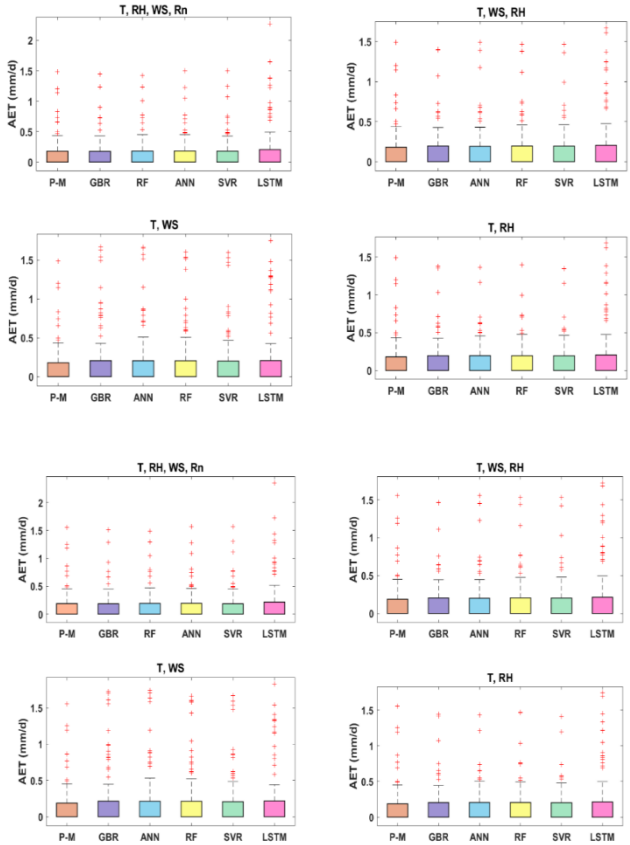

Fig. 5. Comparison of observed and estimated AET using different models (GBR, ANN, LSTM, RF, and SVR) with varying parameters of input for the validation period for Budyko(Top) and Turc methods (Bottom) at Waipara station for penman monteith method.

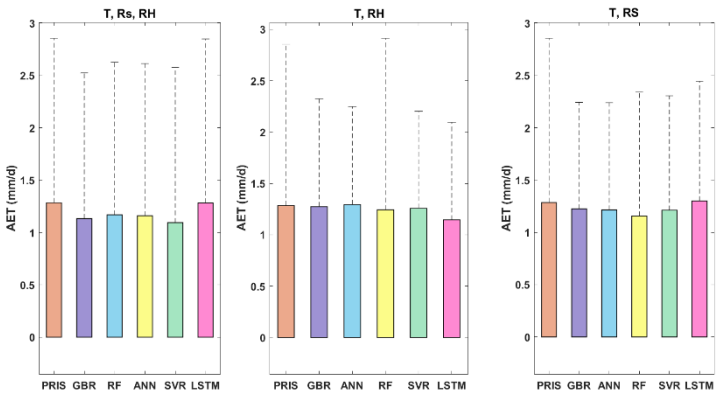

Fig. 6. Comparison of observed and estimated AET using different models (GBR, ANN, LSTM, RF, and SVR) with varying parameters of input for the validation period for Budyko(Top) and Turc methods (Bottom) at Hyderabad station for Priestley method.

The performance of these ML models and the two AET methods for the Hargreaves and Turc methods was provided in Tables 6-7 for both the stations. Tables 6-7 demonstrated that the tested models had comparable performance over the two stations. Figures 7-11 show the comparisons between observed AET and model estimated values in the form of a box plot for two AET-based methods under different input combinations for the Hargreaves and Turc methods. From Tables 6-7 the ranking of the models remained the same as Penman-Monteith and Priestley methods. We have observed that when a limited data combination of PET was utilized to estimate AET, the results have been phenomenal, this can be seen in Tables 6-7 for all the methods with their R^2 values ranging from 0.98 to 0.99. During the validation stage at Hyderabad station, the PET using the input combinations like temperature, relative humidity, and wind speed results (MAE: 0.01–0.09 mm⁄d, RMSE:0.01-0.05 mm⁄d, and R^2: 0.98–0.99) played out the best for both the AET methods of Budyko and Turc. Methods using models with temperature and wind speed data as input combinations accomplished low performance (RMSE: 0.56–058 mm⁄d, MAE: 0.17–0.21 mm⁄d and R^2: 0.88–0.90), trailed by methods dependent on temperature and relative humidity input (RMSE: 0.516-0.56 mm⁄d, MAE: 0.15-0.21 mm⁄d and R^2: 0.87- 0.88) for Penman-Monteith method. For the Priestley Taylor method, the AET methods accomplished low performance with temperature and solar radiation as input (RMSE: 0.21–0.31 mm⁄d, MAE: 0.04–0.12 mm⁄d and R^2: 0.865–0.939), followed by dependent on temperature and relative humidity input (RMSE: 0.23–0.31 mm⁄d, MAE: 0.04–0.21mm⁄d and R^2: 0.93–0.97). For Hargreaves and Turc methods, the minimum temperature and solar radiation combination performed the same as all parameters input combinations for both the AET methods. It is worth noting that even for the AET estimates, the models which are blends of temperature data with relative humidity and wind speed, individually, could accomplish preferred performance over models dependent on temperature and relative humidity input. And the combination of temperature and solar radiation could also accomplish excellent performance compared to temperature and relative humidity for the Priestley method. The outcomes demonstrated that the AET methods using PET modelled from LSTM and ANN performed superior to RF, SVR, and GBR, with temperature and wind speed as input combinations. Furthermore, the AET with LSTM model showed the most remarkable performance when temperature, wind speed, and relative humidity data were accessible for the Penman-Monteith method and temperature and solar radiation when used for Priestley, Hargreaves, and Turc methods. Among the five ML models performing in estimating AET, the second-best model was noted as ANN, followed by SVR, RF, and GBR. Hence, LSTM and ANN can be concluded as the best ML models among any input combination which can be employed in calculating AET, whereas other models performed low when the input combinations were reduced. It was also noted that the two AET methods showed similar performance in all the used cases.

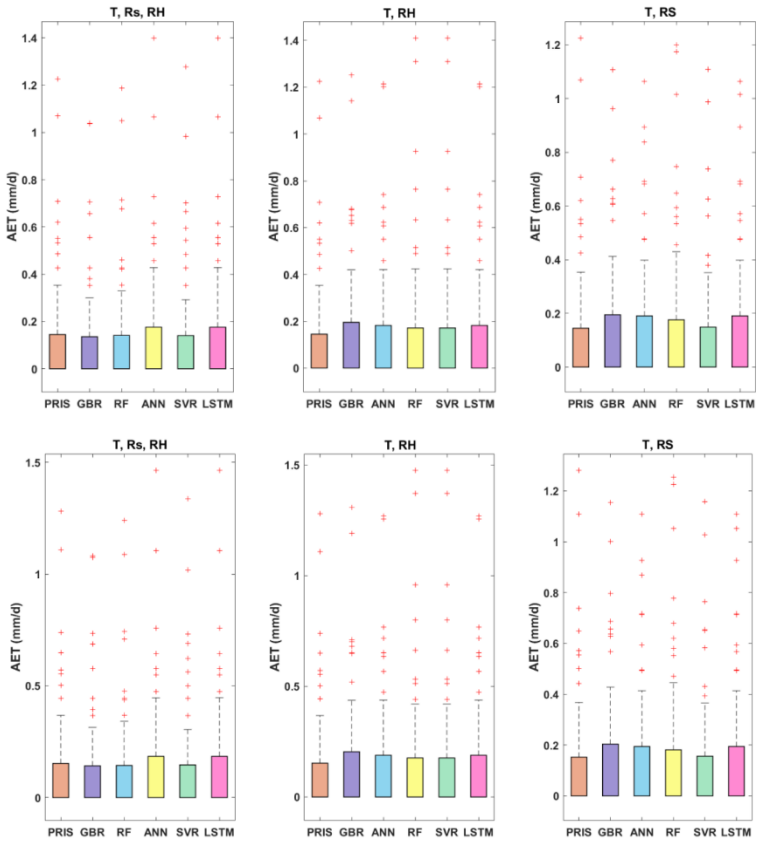

Fig. 7. Comparison of observed and estimated AET using different models (GBR, ANN, LSTM, RF, and SVR) with varying parameters of input for the validation period for Budyko (Top) and Turc methods (Bottom) at Waipara station for Priestley method.

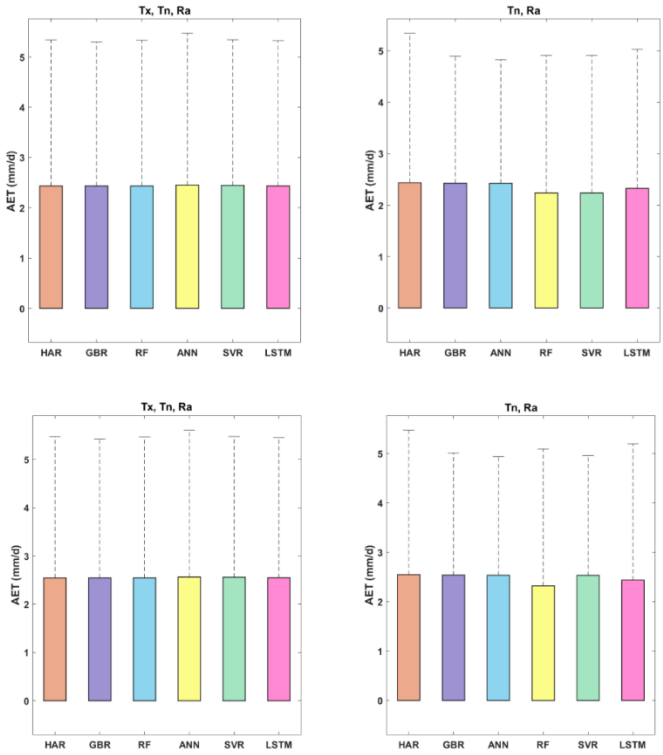

Fig. 8. Comparison of observed and estimated AET using different models (GBR, ANN, LSTM, RF, and SVR) with varying parameters of input for the validation period for Budyko(Top) and Turc methods (Bottom) at Hyderabad station for Hargreaves method.

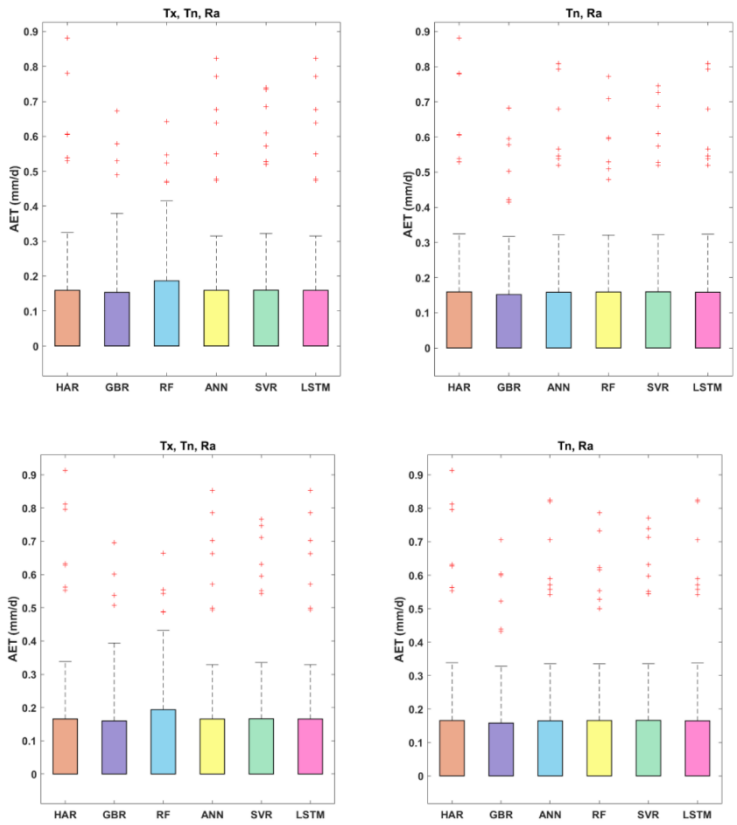

Fig. 9. Comparison of observed and estimated AET using different models (GBR, ANN, LSTM, RF, and SVR) with varying parameters of input for the validation period for Budyko(left) and Turc methods (right) at Waipara station for Hargreaves method.

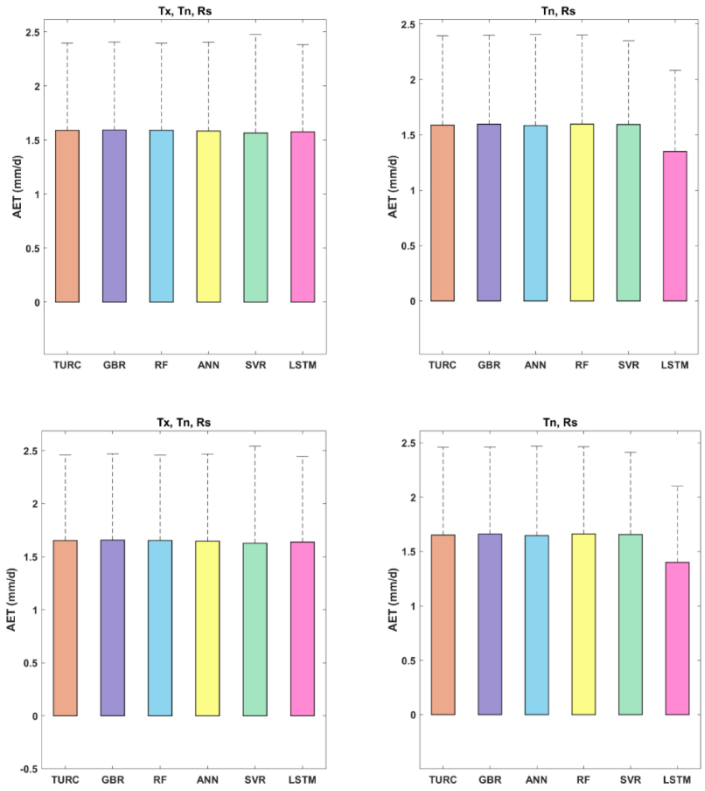

Fig. 10. Comparison of observed and estimated AET using different models (GBR, ANN, LSTM, RF, and SVR) with varying parameters of input for the validation period for Budyko(Top) and Turc methods (bottom) at Hyderabad station for Turc method.

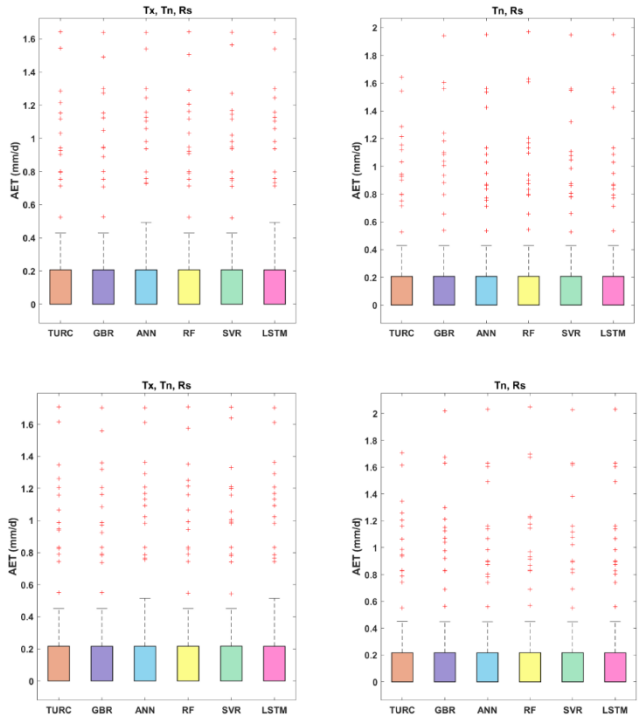

Fig. 11. Comparison of observed and estimated AET using different models (GBR, ANN, LSTM, RF, and SVR) with varying parameters of input for the validation period for Budyko(Top) and Turc methods (bottom) at Waipara station for Turc method.

It was also observed that both AET methods, the results for the Penman-Monteith method were followed by the Priestley method. In Hargreaves and Turc methods, the inputs being the same, AET estimated using the Turc method has shown much better performance under limited combinations when compared to Hargreaves. It was also confirmed that the Turc and Hargreaves method combination showed better performance in estimating AET when compared to the Priestley method. Tables 4-7 showed the summary of the Budyko and Turc based AET estimates using modelled PET at Waipara station. The performance ranking of different ML models and AET methods was like the Hyderabad station, whereas the LSTM performed the best and RF as the worst. AET estimated using PET from all parameters as input combinations performed better compared to other input combinations with its results ranging from (RMSE: 0.01–0.242 mm⁄d, MAE: 0.02-0.07 mm⁄d and R^2: 0.98–0.990). During the validation stage at Waipara station, the different input combinations like temperature, relative humidity, and wind speed (RMSE: 0.01–0.59 mm⁄d, MAE: 0.02–0.08 mm⁄d and R^2: 0.77–0.85) played out the best in estimating AET for Penman-Monteith method and temperature, relative humidity, and solar radiation (RMSE: 0.01–0.561 mm⁄d, MAE: 0.05–0.09 mm⁄d and R^2: 0.76–0.84) played out the best for the Priestley method. In Hargreaves and Turc methods, the performances of all input combinations were the same, though the AET resulting from ANN, and LSTM performed much better than GBR and RF models. Hence, it is recommended to use either of these two PET models in estimating AET. Considering the above-observed results from Tables 4-7 and Figures 4-11, the AET estimated using LSTM and ANN models are the most robust among the five ML modelled PET regardless of under which station or input combination, trailed by SVR and GBR modelled PET, which could accomplish agreeable accuracy in estimating AET. LSTM and ANN are both able to simulate AET where meteorological information is inadequate. Both the AET methods of Budyko and Turc gave an outstanding performance. It can be concluded that the different ML modelled PET estimates employed in estimating AET at two different stations have performed promising when compared to the standard ET estimates. Overall, with respect to the ML models, it can be concluded that ANN and LSTM can be preferred to model PET and AET with all parameters input combination as the first preference followed by three parameters input combination and then two parameters input combination. It can also be

revealed that AET is sensitive to the number of input parameters used in the PET estimation. It is also worth noticing that the accuracy of the AET (Budyko and Turc) methods with all parameters input combinations was the highest in each station. However, one can use the three input combination parameters or the two input combination parameters (e.g., temperature and relative humidity or temperature and wind speed) in PET and AET estimations under limited data. This study has attempted to estimate AET from ML-modelled PET and concluded that this could be used in the future for different case studies. Using the five different ML models: ANN, LSTM, GBR, SVR, RF, and different empirical methods, different AET estimates were developed. The models were analysed and compared in terms of prediction accuracy, generalization ability, complexity/simplicity of the modelling approach, and model usage. The comparison was conducted to identify the most efficient technique out of the studied five ML techniques to predict the PET in developing AET estimates. The results of the ML models were compared with those of the five empirical methods and two AET modelled methods to identify the possible advantages of the proposed models over one of the available methods for the estimation of AET under limited data. Although the generated models, based on error measures, are performing well and are similar, they use different combinations of inputs with different mathematical structures. This demonstrates that precise identification of the hydrometeorological variables driving the AET process is not a straightforward task, where different combinations of inputs may result in good AET estimates. Among the proposed models in this study, Budyko and Turc are both equation-based methods. Such explicit equation-based methods are more appealing to hydrological implementations for ungauged basins because of the transparency and the simplicity of their application. The meteorological variables that were observed to have the most significant contribution in modelling PET were the same for AET methods. This was observed using five different ML models, which could capture the most relevant meteorological variables. According to the observed two AET methods, the meteorological variables that were found to be most important in predicting AET (large-scale) were net precipitation, radiation, and temperature. Radiation is a well-known variable that serves as an energy source and is one of the critical components of the ET mechanism. The surface soil moisture, surface soil temperature, and turbulent sensible heat flux are a few other essential elements that shape the physics of AET (Wang et al., 2017). The physical description of the AET mechanism explains the importance of soil moisture and its complex interaction with other land-atmosphere variables in the AET process at daily time scales (Dingman, 2015; Wang et al., 2017). It was interesting to investigate the level of cause and relationship between meteorological variables such as temperature, relative humidity, solar radiation, and wind speed involved in AET variations. To make this comparison, the time series of PET and AET using temperature, relative humidity, solar radiation, and wind speed were visually compared over a typical time window. The comparison was carried out on daily time series data for both stations. It can be concluded that temperature varies slightly over time compared to other variables. It can also be noted that the temperature and solar radiation gradually decrease over time, resulting in a lower value. As a result, precipitation and temperature influence the AET estimation over a daily time scale. Because the process of AET is not fully understood, it is challenging to mechanistically capture the interactions that exist among the state variables to present a mathematical relationship between AET and highly correlated meteorological variables. Explicit ML models demonstrated their ability to efficiently capture PET variations in estimating AET and to induce symbolic estimation models, which are primarily dominated by net radiation, temperature, and wind speed.

4. Conclusion

The AET over semi-arid climatic conditions of Hyderabad, Telangana, (India), and Waipara (New Zealand) was estimated using ML modelled PET with different empirical methods using Budyko and Turc methods. The Penman-Monteith model-based AET was considered as the standard reference method. The daily AET values were estimated using PET obtained from five different ML techniques, namely LSTM, ANN, SVR, GBR and RF, using different input combinations. The four input variable combinations such as maximum and minimum

air temperature, relative humidity, solar radiation, and wind speed; three input variable combinations such as average air temperature, relative humidity, and solar radiation; two input variable combinations such as temperature and solar radiation; and temperature and wind speed. The study investigated that the best performance was when all input variable combinations were used. However, the study also found that even three input variable combinations or two combination input variable combinations can provide identical results. The study also investigated that the two methods Turc and Budyko performed equally well with good R^2 values. The results were discussed and compared with the results of alternative methods of PET calculation, such as the radiation-based methods of Priestly-Taylor, the temperature-based methods of Hargreaves, and Turc. The correlation coefficient values suggest that precipitation and temperature are the most crucial factors, followed by solar radiation, wind speed, and relative humidity, respectively for both regions. For both the regions, LSTM and ANN were found to be more effective than the other techniques in identifying the most relevant meteorological predictors. It can be concluded that for the two regions, temperature and solar radiation have a maximum correlation with AET estimates of Penman-Monteith models compared to relative humidity and wind speed. The Turc model used temperature and solar radiation as input variables and showed high accuracy with all ML models in estimating AET. In contrast, relative humidity has the least correlation with the AET estimates. Due to the lower dependency of relative humidity on the AET estimates, the Priestly-Taylor model has lower accuracy than ML models compared to the Turc model. The results also showed that the AET obtained from PET using LSTM and ANN models could offer the most remarkable performance among four tested models regardless of station or input combination, trailed by SVR and GBR models, which could likewise accomplish moderately reliable performance. The study concludes that the empirical models work well with data-driven algorithms that consider the climate variables have a high dependency on the standard PET estimates in calculating AET. Such studies can be implemented for the development of ML models statistically dependent on PET in AET estimates. The study demonstrated that the modelling of PET through the LSTM and ANN techniques gave better AET estimates that proved with their performance criterion, i.e., R2 as 0.99. The study concluded that the performance of the AET methods varies according to the number of inputs and the predicted time step. Overall, results are of significant practical use when limited climate data is available 85 to estimate the AET. So, it can be concluded that even if not all parameter information is available in a particular station, the three-parameter combination can be used, or the two combinations, which are temperature and wind speed or temperature and relative humidity values, to calculate AET using modelled PET. It was also concluded that the equation-based methods of Budyko and Turc, which were presented in this study, are not the only capacity of the methods as an evolutionary methodology that uses ML techniques. However, they can also be implemented to evolve program-based models and estimate AET in different regions. These ML models effectively determine the best input variables for modelling small- and large-scale PET variations in generating AET. Further, the modelled PET was efficient in estimating AET for two different stations. However, they have the potential to provide deep insight into the larger-scale variations of AET, such as diurnal variations. It should also be noted that no single ML technique can always capture all complex processes. As a result, various techniques may be capable of accurately predicting various challenging components of hydrology.

References

Alexandris, S. & Kerkides, P., 2003. New empirical formula for hourly estimations of reference evapotranspiration. Agric. Water Manag, 60, 157-180. https://doi.org/10.1016/S0378-3774(02)00172-5

Allan, R., Pereira, L. & Smith, M., 1998. Crop evapotranspiration-Guidelines for computing crop water requirements-FAO Irrigation and drainage paper 56.

Amatya, D.M., Skaggs, R.W. & Gregory, J.D., 1995. Comparison of Methods for Estimating REF-ET. *J. Irrig. Drain. Eng*. 121, 427-435. https://doi.org/10.1061/(ASCE)0733-9437(1995)121:6(427)

Asokan, S.M. & Jarsjö, J., 2010. Vapor flux by evapotranspiration: Effects of changes in climate, land use, and water use. *J. Geophys. Res. Atmospheres* 115. https://doi.org/10.1029/2010JD014417

Bastiaanssen, W.G.M., Menenti, M., Feddes, R.A. & Holtslag, A.A.M., 1998. A remote sensing surface energy balance algorithm for land (SEBAL). 1. *Formulation. J. Hydrol*, 212–213, 198–212. https://doi.org/10.1016/S0022-1694(98)00253-4

Biggs, T.W., Mishra, P.K. & Turral, H., 2008. Evapotranspiration and regional probabilities of soil moisture stress in rainfed crops, southern India. Agric. For. Meteorol. 148, 1585–1597. https://doi.org/10.1016/j.agrformet.2008.05.012

Blaney, H.F., 1892, 1952. Determining water requirements in irrigated areas from climatological and irrigation data.

Bray, R.H. & Kurtz, L.T., 1945. Determination of Total, Organic, And Available Forms of Phosphorus in Soils. Soil Sci. 59, 39-46.

Budyko, M.I., 1961. The Heat Balance of the Earth's Surface. Sov. Geogr. 2, 3-13. https://doi.org/10.1080/00385417.1961.10770761

Silva, C.D.O.F., & Manzione, R.L., 2021. Modelagem Espacial Da Evapotranspiracao Em Agroecossistema Do Sistema Aquifero Bauru | Águas Subterrâneas [WWW Document]. URL https://aguassubterraneas.abas.org/asubterraneas/article/view/29356 (accessed 4.23.22).

Chow, V.T., 2010. Applied Hydrology. Tata McGraw-Hill Education.

Deo, R.C. & Samui, P., 2016. Estimation of monthly evaporative loss using relevance vector machine, extreme learning machine and multivariate adaptive regression spline models. Stoch. Environ. Res. Risk Assess. 30, 1769-1784. https://doi.org/10.1007/s00477-015-1153-y

Dingman, S.L., 2015. Physical Hydrology: Third Edition. Waveland Press.

Fu, B.P., 1981. Fu, B.P. (1981) On the Calculation of the Evaporation from Land Surface. Scientia Atmospherica Sinica, 5, 23-31. - References - Scientific Research Publishing [WWW Document]. URL https://www.scirp.org/%28S%28vtj3fa45qm1ean45vvffcz55%29%29/reference/referencespapers.aspx?referenceid=1185500 (accessed 4.23.22).

Geigy, R., Jenni, L., Kauffmann, M., Onyango, R.J. & Weiss, N., 1975. Identification of T. brucei-subgroup strains isolated from game. Acta Trop. 32, 190-205.

Gudulas, K., Voudouris, K., Soulios, G. & Dimopoulos, G., 2013. Comparison of different methods to estimate actual evapotranspiration and hydrologic balance. Desalination Water Treat. 51, 2945-2954. https://doi.org/10.1080/19443994.2012.748443

Hargreaves, G. & Samani, Z., 1985. Reference Crop Evapotranspiration From Temperature. Appl. Eng. Agric. 1. https://doi.org/10.13031/2013.26773

Jensen, M.E., Allen, R.G., Walter, I.A., Elliott, R., Mecham, B., Itenfisu, D., Howell, T.A., Snyder, R., Brown, P., Echings, S., Spofford, T., Hattendorf, M., Cuenca, R.H., Wright, J.L. & Martin, D., 1990. Issues, Requirements and Challenges in Selecting and Specifying a Standardized Et Equation.

Jensen, M.E., Walter, I.A., Allen, R.G., Elliott, R., Itenfisu, D., Mecham, B., Howell, T.A., Snyder, R., Brown, P., Echings, S., Spofford, T., Hattendorf, M., Cuenca, R.H., Wright, J.L. & Martin, D., 2012. ASCE's Standardized Reference Evapotranspiration Equation 1-11. https://doi.org/10.1061/40499(2000)126.

Landeras, G., Ortiz-Barredo, A. & López, J.J., 2008. Comparison of artificial neural network models and empirical and semi-empirical equations for daily reference evapotranspiration estimation in the Basque Country (Northern Spain). Agric. Water Manag. 95, 553-565. https://doi.org/10.1016/j.agwat.2007.12.011

Leith, C.E., 1975. Climate Response and Fluctuation Dissipation. J. Atmospheric Sci. 32, 2022-2026. https://doi.org/10.1175/1520-0469(1975)032<2022:CRAFD>2.0.CO;2

Ma, X., Zhao, Q., Yao, Y. & Yao, W., 2021. A novel method of retrieving potential ET in China. J. Hydrol. 598, 126271. https://doi.org/10.1016/j.jhydrol.2021.126271

Magliulo, V., d'Andria, R. & Rana, G., 2003. Use of the modified atmometer to estimate reference evapotranspiration in Mediterranean environments. Agric. Water Manag. 63, 1-14. https://doi.org/10.1016/S0378-3774(03)00098-2

McVicar, T.R., Roderick, M.L., Donohue, R.J. & Van Niel, T.G., 2012. Less bluster ahead? Ecohydrological implications of global trends of terrestrial near-surface wind speeds. Ecohydrology 5, 381-388. https://doi.org/10.1002/eco.1298

Pereira, A.R. & Pruitt, W.O., 2004. Adaptation of the Thornthwaite scheme for estimating daily reference evapotranspiration. Agric. Water Manag. 66, 251-257. https://doi.org/10.1016/j.agwat.2003.11.003

Priestley, C.H.B. & Taylor, R.J., 1972. On the Assessment of Surface Heat Flux and Evaporation Using Large-Scale Parameters. Mon. Weather Rev. 100, 81-92. https://doi.org/10.1175/1520-0493(1972)100<0081:OTAOSH>2.3.CO;2

Rim, C.S., 2008. Estimating evapotranspiration from small watersheds using a water and energy balance approach. *Hydrol. Process.* 22, 703-714. https://doi.org/10.1002/hyp.6769

Naoum, S. and Tsanis, I., 2003. Hydroinformatics in evapotranspiration estimation - ScienceDirect [WWW Document]. URL https://www.sciencedirect.com/science/article/pii/S1364815202000762 (accessed 4.23.22).

Su, T., Xie, D., Feng, T., Huang, B., Qian, Z., Feng, G. & Wu, Y., 2022. Quantifying the contribution of terrestrial water storage to actual evapotranspiration trends by the extended Budyko model in Northwest China. Atmospheric Res. 273, 106147. https://doi.org/10.1016/j.atmosres.2022.106147

Su, Z., 2002. The Surface Energy Balance System (SEBS) for estimation of turbulent heat fluxes. Hydrol. Earth Syst. Sci. 6, 85-100. https://doi.org/10.5194/hess-6-85-2002

Turc, L., 1961. Estimation of irrigation water requirements, potential evapotranspiration: a simple climatic formula evolved up to date. Ann. Agron, 12(1), 13-49.

Turc, L., 1954. The water balance of soils. Relation between precipitation, evaporation and flow.

Utset, A., Farré, I., Martínez-Cob, A. & Cavero, J., 2004. Comparing Penman–Monteith and Priestley–Taylor approaches as reference-evapotranspiration inputs for modeling maize water-use under Mediterranean conditions. Agric. Water Manag. 66, 205-219. https://doi.org/10.1016/j.agwat.2003.12.003

Walter, I.A., Allen, R.G., Elliott, R., Jensen, M.E., Itenfisu, D., Mecham, B., Howell, T.A., Snyder, R., Brown, P., Echings, S., Spofford, T., Hattendorf, M., Cuenca, R.H., Wright, J.L. & Martin, D., 2012. ASCE's Standardized Reference Evapotranspiration Equation 1-11. https://doi.org/10.1061/40499(2000)126

Wang, Z., Wu, J., Liu, C. & Gu, G., 2017. Integrated Assessment Models of Climate Change Economics. Springer, Singapore. https://doi.org/10.1007/978-981-10-3945-4

Zhang, L., Potter, N., Hickel, K., Zhang, Y. & Shao, Q., 2008. Water balance modeling over variable time scales based on the Budyko framework – Model development and testing. J. Hydrol. 360, 117-131. https://doi.org/10.1016/j.jhydrol.2008.07.021

Zheng, Z., Gao, J., Ma, Z., Wang, Z., Yang, X., Luo, X., Jacquet, T. & Fu, G., 2016. Urban flooding in China: main causes and policy recommendations. Hydrol. Process. 30, 1149-1152. https://doi.org/10.1002/hyp.10717.